BIOLOGY, MEDICINE, & NATURAL PRODUCT CHEMISTRY ISSN 2089-6514 (paper)
Volume 14, Number 1, April 2025 | Pages: 541-552 | DOI: 10.14421/biomedich.2025.141.541-552 ISSN 2540-9328 (online)

Antimicrobial Potential of Phytochemicals from *Coccinia grandis* Leaves: A Molecular Docking Study Against Penicillin-Binding Protein 5 of *Escherichia coli* and DNA Topoisomerase IV Subunit B (ParE 24kDa) of *Staphylococcus aureus* and *Escherichia coli*

Malshan Isuranga*, Dulki Nihinsa Danthanarayana
Faculty of Science, University of Kelaniya, Sri Lanka.

Corresponding author*
malshanisuranga98@gmail.com

Manuscript received: 06 February, 2025. Revision accepted: 20 May, 2025. Published: 04 August, 2025.

Abstract

Coccinia grandis (*C. grandis*) leaves, traditionally used in Sri Lanka for diabetes management, also have a potential antimicrobial activity. In this study, site-specific molecular docking was performed to investigate the antimicrobial activity of phytochemicals of *Coccinia grandis* leaves against Penicillin-binding protein 5 (PBP 5) and DNA topoisomerase IV subunit B (ParE 24kDa) of *Escherichia coli* (*E. coli*) and DNA topoisomerase IV subunit B (ParE 24kDa) of *Staphylococcus aureus* (*S. aureus*). Penicillin was selected as the reference molecule for Penicillin-binding protein 5 and for DNA topoisomerase IV subunit B (ParE 24kDa), Novobiocin was selected as the reference molecule. The results identified Lupeol (-7.72 kcal/mol) and Beta-Sitosterol (-8.21kcal/mol) have a higher binding affinity to PBP5 of *E. coli* than Penicillin (-7.20 kcal/mol). Quercetin (-6.70 kcal/mol), Kaempferol (-6.95 kcal/mol), Naringenin (-7.07 kcal/mol), Isoquercetin (-6.15 kcal/mol), Lupeol (-7.87 kcal/mol), Beta-Sitosterol (-9.42 kcal/mol) and Sanguinarine (-9.07 kcal/mol) show higher binding affinity to DNA topoisomerase IV subunit B (ParE 24kDa) of *S. aureus* than novobiocin (-6.04 kcal/mol). As well Quercetin (-6.85 kcal/mol), Kaempferol (-6.82 kcal/mol), Naringenin (-7.23 kcal/mol), Isoquercetin (-6.20 kcal/mol), Lupeol (-7.67 kcal/mol), Beta-Sitosterol (-9.08 kcal/mol) and Sanguinarine (-9.03 kcal/mol) show higher binding affinity to DNA topoisomerase IV subunit B (ParE 24kDa) of *E. coli* than novobiocin (-5.76 kcal/mol). In silico pharmacokinetic and physicochemical parameter predictions were also conducted to study drug-likeness of above molecules using specialized web servers.

Keywords: *Coccinia grandis*; *Escherichia coli*; *Staphylococcus aureus*; Penicillin-Binding Protein 5; DNA topoisomerase IV subunit B (ParE 24kDa); Molecular Docking.

INTRODUCTION

Antibiotics are the most wonderful innovation in the history of medicine. From the first antibiotic, Penicillin, discovered by Alexander Fleming in 1928, antibiotics have a long development history. These drugs have saved numerous numbers of lives worldwide. Some antibiotics kill the microorganisms while others reduce their growth rate.

Antibiotic Resistance (ABR) is the ability of microorganisms to withstand the activity of the antibiotic. Mutations, Horizontal Gene Transfer, and Human Actions such as misuse of antibiotics contribute to the ABR (Larsson & Flach, 2022). According to the World Health Organization (WHO), ABR is one of the most significant global health threats (*Global Antimicrobial Resistance and Use Surveillance System (GLASS) Report 2022*, 2022).

Coccinia grandis belongs to the family Cucurbitaceae, predominantly distributed in tropical Asia and Africa including Pakistan, India, and Sri Lanka (Farrukh et al., 2008). *C. grandis* is commonly known as Ivy Gourd or Scarlet Gourd in English; Kowakka in Sinhala. In Sri Lanka, this plant is predominantly distributed in the North Central, Southern, and Western regions. From centuries local population of Sri Lanka used leaves of this plant for diabetes management (Attanayake et al.,2016). Researchers suggest that leaf extract of *C. grandis* exhibits Anti-hyperglycemic, Xanthine Oxidase inhibitory, Analgesic, Anti-inflammatory, Antipyretic, Antioxidant, Anti-hyperlipidemic, Antimicrobial, and Anti-hepatotoxic activities (Ramachandran et al., 2014).

Penicillin-binding protein 5 (PBP 5) of *E. coli* engages in cell wall synthesis. The main constituent of the bacterial cell wall is Peptidoglycan. PBP 5 enzyme performs a DD-carboxypeptidase reaction on the bacterial Peptidoglycan. The active site of PBP 5 contains a specific serine residue, which acts like a hook to grab a unit of the Peptidoglycan chain during the

enzymatic reaction. Near the active site, two lysine residues (Lys47 and Lys213) play a critical role in proton-transfer events during acylation and deacylation events (Zhang et al., 2007).

PBP 5 can be inactivated by β-lactam antibiotics such as penicillin. Inactivation occurs when the antibiotic forms a covalent bond with a serine residue in PBP 5, creating a stable complex that inhibits the protein's enzymatic activity and disrupts its normal function. When PBP 5 binds to the antibiotic, it is dormant in an acylation state, thus, disrupting the cell wall synthesis, and resulting in cell death (Nicholas et al., 2003).

DNA topoisomerase IV subunit B (ParE 24kDa) of *Escherichia coli* (*E. coli*) is an important enzyme that regulates DNA topology during replication and transcription. Its primary role is to separate the intertwined daughter chromosomes after DNA replication, ensuring that genetic material is correctly distributed to daughter cells. ParE functions with another subunit, ParC, to form a heterotetrameric complex (C2E2) that utilizes the energy derived from ATP hydrolysis to introduce and relax supercoils in DNA (Bellon et al., 2004).

MATERIALS AND METHODS

Ligand Preparation:

Phytochemicals of *Coccinia grandis* leaves identified through a literature survey. The structure of the active site of *E. coli* PBP 5 was also obtained through literature survey. The structures of selected molecules obtained from PubChem database (*PubChem*, n.d.) in .sdf format. The energy-minimization of ligands was performed using Avogadro (version 1.2.0) software and saved in .pdb format.

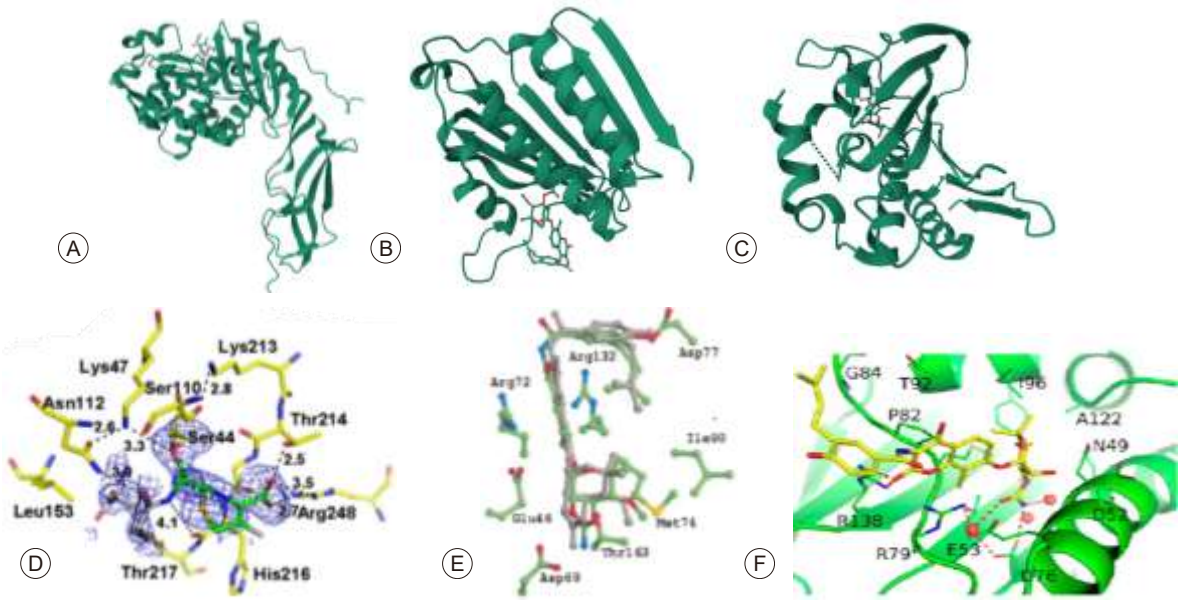

Figure 1. (**A)** Crystal structure of *Escherichia coli* PBP 5 in complex with a peptide-mimetic penicillin **PDB DOI:** https://doi.org/10.2210/pdb3BEB/pdb, (**B)** Crystal structure of *E. coli* Topoisomerase IV ParE 24kDa subunit **PDB DOI:** https://doi.org/10.2210/pdb1S14/pdb, **(C)** Crystal Structure of *S. aureus* ParE 24kDa in complex with Novobiocin **PDB DOI:** https://doi.org/10.2210/pdb4URN/pdb, (**D)** Structure of active site of *E. coli* PBP 5 (Sauvage et al., 2008), (**E)** Structure of active site of *E. coli* ParE 24kDa (Bellon et al., 2004) (**F)** Structure of active site of *S. aureus* ParE 24kDa (Lu et al., 2014b).

Protein Preparation:

The crystal structures of proteins were obtained from protein data bank in .pdb format (PDB **ID – 3BEB**: Crystal structure of *E. coli* penicillin-binding protein 5 in complex with a peptide-mimetic penicillin - PDB DOI: https://doi.org/10.2210/pdb3BEB/pdb (Sauvage et al., 2008), **PDB ID – 1S14**: Crystal structure of *Escherichia coli* Topoisomerase IV ParE 24kDa subunit - PDB DOI: https://doi.org/10.2210/pdb1S14/pdb (Bellon et al., 2004), **PDB ID – 4URN**: Crystal Structure of *Staph* ParE 24kDa in complex with Novobiocin – PDB DOI: https://doi.org/10.2210/pdb4URN/pdb (Lu et al., 2014).

The protein was prepared using AutodockTools (version 1.5.7). Heteroatoms and water molecules were removed, and Polar hydrogen and Kollman chargers were added to the protein. AD4 type atoms were assigned to the protein.

Molecular Docking:

Autodock version 4.2.6 was used to perform site-specific molecular docking and results were generated in .dlg format (output – LamarckianGA-4.2). The grid parameters were set to cover the active site of each protein complex.

Table 1. Grid map dimensions (A^0) and Grid-center coordinates (A^0).

Protein Complex	Grid map dimensions (A^0)			Grid-center coordinates (A^0)		
	x-axis	y-axis	z-axis	x-axis	y-axis	z-axis
***E. coli* PBP 5**	15.8	26.3	16.5	42.732	4.638	26.112
***E. coli* ParE 24kDa subunit**	18.0	18.0	17.3	19.236	26.093	48.526
***Staph* ParE 24kDa subunit**	17.3	21.0	19.5	-27.52	5.92	0.958

The genetic algorithm (GA) parameters were set to 50 runs with 300 population size. The maximum number of evaluations: 25,000,000 (medium) and maximum number of generations 27 000 (Lawan & Tharakee, 2023).

Molecular dynamics simulation:

The site-specific molecular docking results were analyzed using Autodocktools (Version 1.5.7). Binding energies and Inhibition constants were examined,and the interactions were visualized using Discovery studio visualizer (v24.1.0.23298).

Drug-likeness and Pharmacokinetics of Selected Molecules:

The potential of selected molecules as drugs was evaluated by assessing their drug-likeness and pharmacokinetic properties.

Pharmacokinetics parameters of the selected molecules were predicted using the PkCSM server (https://biosig.lab.uq.edu.au/pkcsm/prediction) and SwissADME (http://www.swissadme.ch/index.php). These parameters describe how a drug behaves in the body including absorption, distribution, metabolism, excretion, and toxicity (Table 9).

The drug-likeness of the molecules was analyzed using SwissADME (http://www.swissadme.ch/index.php), which evaluates molecules against Lipinski's rule of five (Lipinski et al., 2001) and Verber's rules (Veber et al., 2002) (Table 8).

Docking Validation (Quality control):

The docking procedure was validated by removing the inhibitor from each obtained protein complex and re-docking the inhibitor. The re-docked complex was aligned with the reference crystalized complex using PyMOL (version 2.5.8), and the difference in their positions was measured using the root mean square deviation (RMSD) (Shivanika et al., 2022).

RESULTS

Table 2. Calculated Binding Energies and Inhibition Constants of Selected Molecules against PBP 5 of *E. coli.*

Molecule	Reference RMSD (A^0)	Binding Energy (kcal/mol)	Inhibition Constant-Ki (μM) at 298.15 K
Penicillin	51.41	-7.20	5.32
Quercetin	49.21	-6.19	28.88
Kaempferol	49.70	-5.90	47.19
Naringenin	51.17	-6.27	25.47
Isoquercetin	51.46	-6.08	34.69
Lupeol	49.67	-7.72	2.19
Beta-Sitosterol	47.94	-8.21	0.953
Rutin	50.44	-5.24	143.35
Sanguinarine	48.95	-6.53	16.23
p-Coumaric Acid	Unsuccessful		

Table 3. Calculated Binding Energies and Inhibition Constants of Selected Molecules against Topoisomerase IV ParE 24kDa subunit of *E. coli.*

Molecule	Reference RMSD (A^0)	Binding Energy (kcal/mol)	Inhibition Constant-Ki (μM) at 298.15 K
Novobiocin	57.21	-5.76	60.25
Quercetin	60.87	-6.85	9.45
Kaempferol	60.68	-6.82	10.08
Naringenin	60.92	-7.23	5.01
Isoquercetin	60.71	-6.20	28.57
Lupeol	59.13	-7.67	2.39
Beta-Sitosterol	58.98	-9.08	222.53
Rutin	58.62	-4.38	611.52
Sanguinarine	60.40	-9.03	0.241
p-Coumaric Acid	Unsuccessful		

Table 4. Calculated Binding Energies and Inhibition Constants of Selected Molecules against Topoisomerase IV ParE 24kDa subunit of *S. aureus.*

Molecule	Reference RMSD (A^0)	Binding Energy (kcal/mol)	Inhibition Constant-Ki (μM) at 298.15 K
Novobiocin	25.79	-6.04	37.19
Quercetin	24.15	-6.70	12.27
Kaempferol	25.23	-6.95	7.99
Naringenin	23.41	-7.07	6.63
Isoquercetin	25.88	-6.15	31.28
Lupeol	26.02	-7.87	1.70
Beta-Sitosterol	23.93	-9.42	0.125
Rutin	26.99	-5.42	106.89
Sanguinarine	23.39	-9.07	0.224
p-Coumaric Acid		Unsuccessful	

Figure 2. (**A)** Superimposition of re-docked penicillin (yellow) on active site of crystalized structure (Green) of *Escherichia coli* PBP 5 using PyMOL (RMSD = 0.000 A^0), (**B)** Superimposition of re-docked novobiocin (yellow) on active site of crystalized structure (Green) of *E. coli* Topoisomerase IV ParE 24kDa subunit using PyMOL (RMSD = 0.000 A^0), **(C)** Superimposition of re-docked novobiocin (yellow) on active site of crystalized structure (Green) of *S. aureus* ParE 24kDa using PyMOL (RMSD = 0.000 A^0).

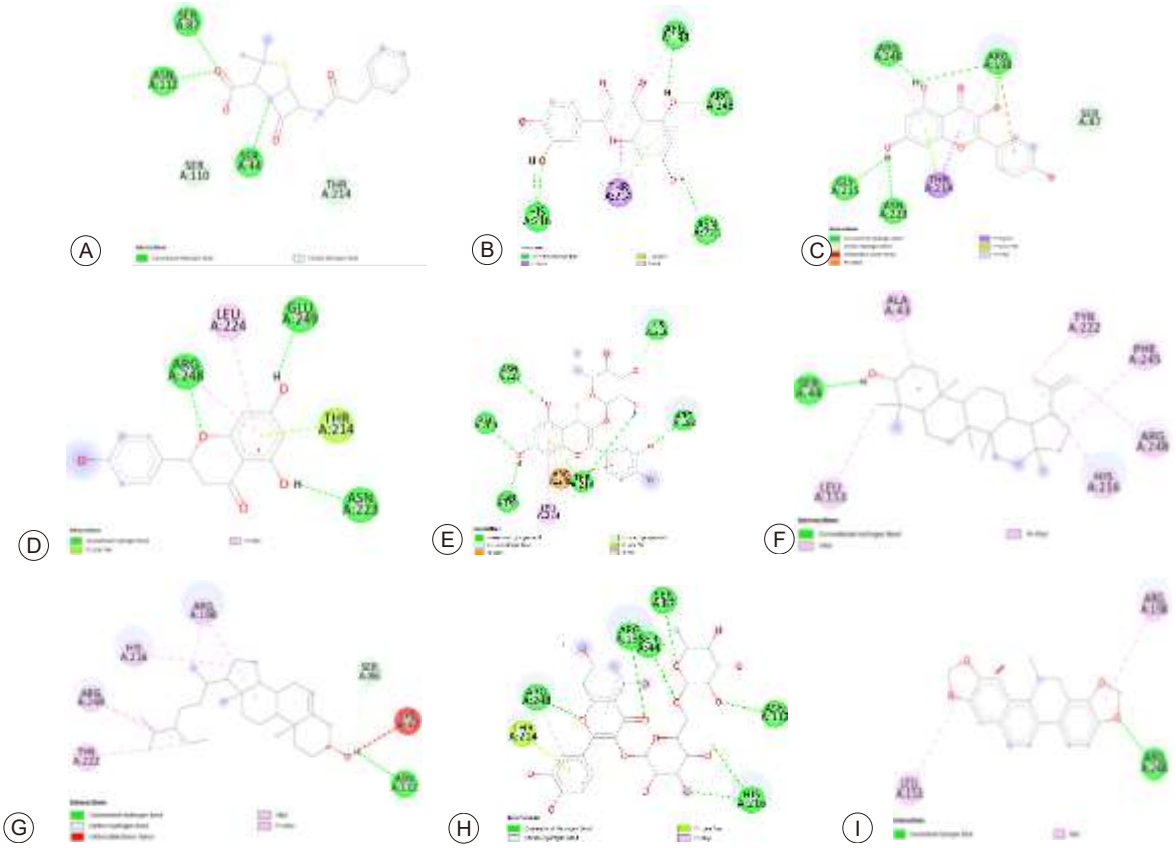

Figure 3. Interactions between selected molecules and *Escherichia coli* PBP 5 **(A)** Penicillin, **(B)** Quercetin, **(C)** Kaempferol, **(D)** Naringenin, (**E)** Isoquercetin, **(F)** Lupeol, **(G)** Beta-Sitosterol, **(H)** Rutin, **(I)** Sanguinarine

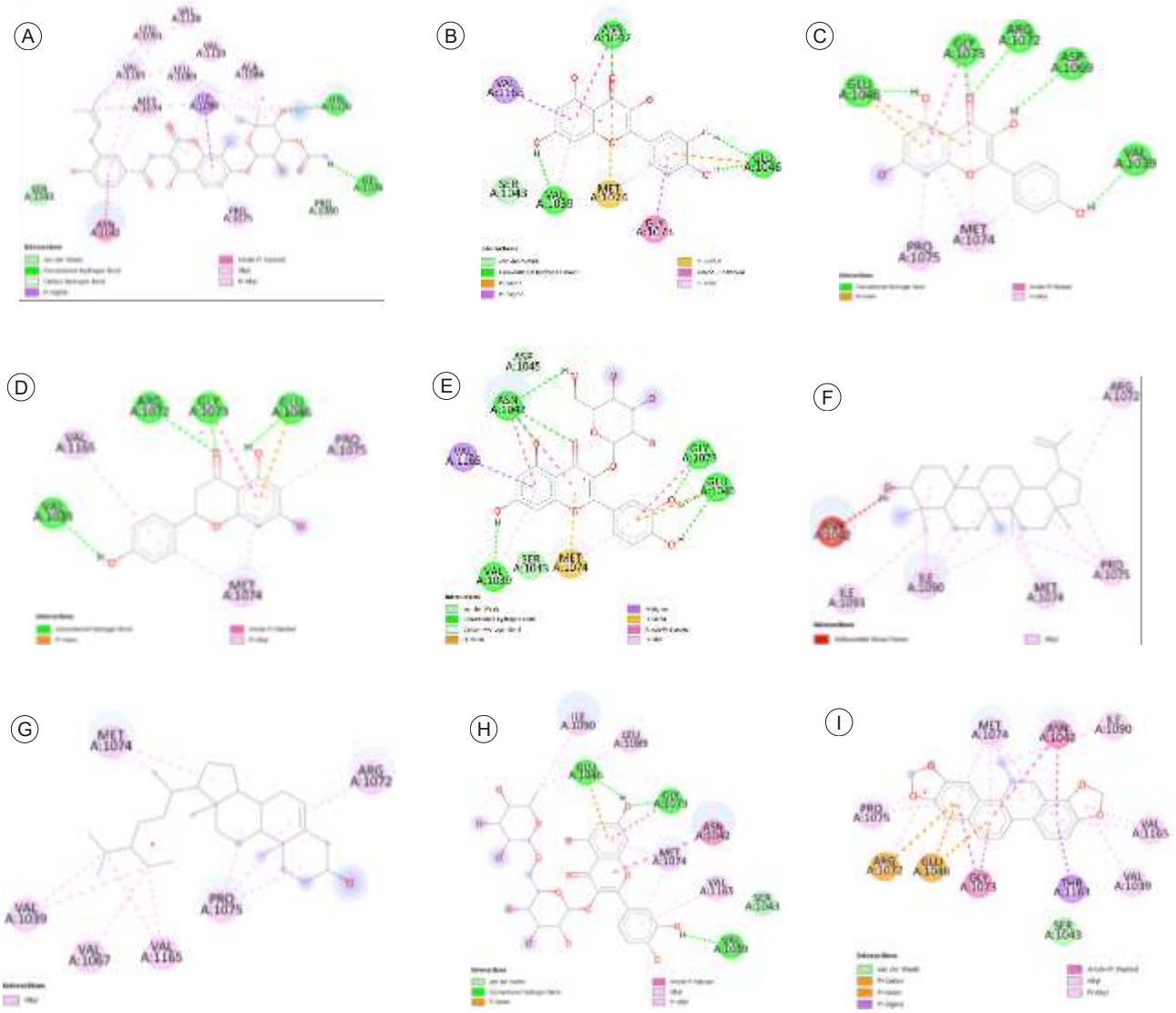

Figure 4. Interactions between selected molecules and Topoisomerase IV ParE 24kDa subunit of *E. coli* **(A)** Novobiocin, **(B)** Quercetin, **(C)** Kaempferol, **(D)** Naringenin, (**E)** Isoquercetin, **(F)** Lupeol, **(G)** Beta-Sitosterol, **(H)** Rutin, **(I)** Sanguinarine.

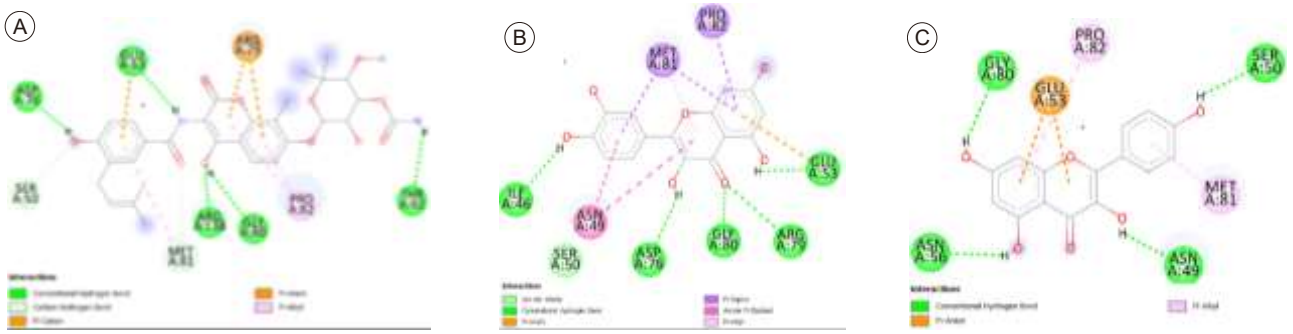

Figure 5. Interactions between selected molecules and Topoisomerase IV ParE 24kDa subunit of *S. aureus* **(A)** Novobiocin, **(B)** Quercetin, **(C)** Kaempferol, **(D)** Naringenin, (**E)** Isoquercetin, **(F)** Lupeol, **(G)** Beta-Sitosterol, **(H)** Rutin, **(I)** Sanguinarine.

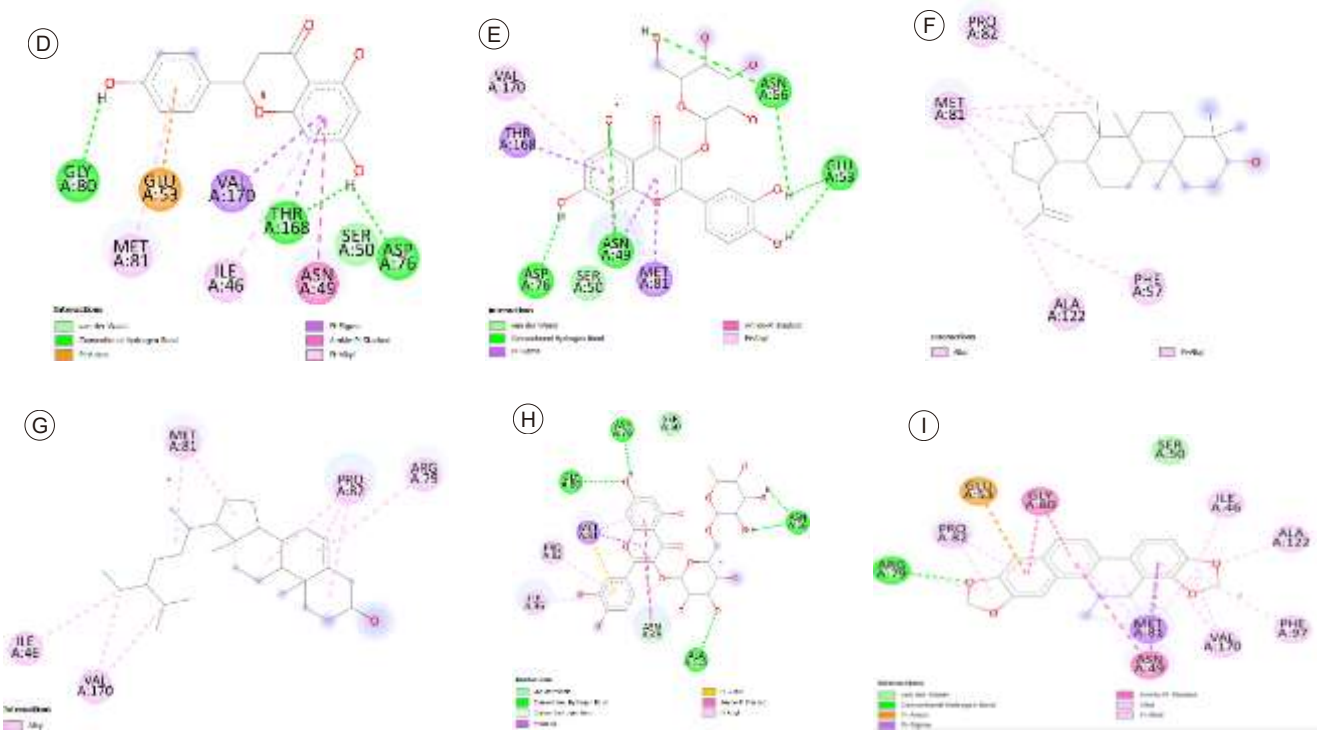

Figure 5. *Cont*.

Table 5. Hydrogen bonding interactions (Intermolecular Conventional Hydrogen Bond) between ligands and PBP 5 of *E. coli*.

Molecule	Name	Distance (A^0)	H-Donor	H-Acceptor	DHA Angle (^{0})
Penicillin	A:SER44:HG - :UNL1:N	1.70075	A:SER44:HG	:UNL1:N	153.622
	A:SER87:HN - :UNL1:OXT	2.15591	A:SER87:HN	:UNL1:OXT	163.07
	A:ASN112:HD21 - :UNL1:OXT	2.10638	A:ASN112:HD21	:UNL1:OXT	159.893
Lupeol	:UNL1:H - A:SER44:OG	1.90396	:UNL1:H	A:SER44:OG	147.908
Beta-Sitosterol	:UNL1:H - A:ASN112:OD1	2.42915	:UNL1:H	A:ASN112:OD1	137.911

Table 6. Hydrogen bonding interactions (Intermolecular Conventional Hydrogen Bond) between ligands and Topoisomerase IV ParE 24kDa subunit of *E. coli*.

Molecule	Name	Distance (A^0)	H-Donor	H-Acceptor	DHA Angle (^{0})
Novobiocin	A:HIS1079:HE2 - :UNL1:O	2.89395	A:HIS1079:HE2	:UNL1:O	112.624
	:UNL1:H - A:ILE1078:O	2.44228	:UNL1:H	A:ILE1078:O	176.688
Quercetin	A:ASN1042:HD21 - :UNL1:O	2.88793	A:ASN1042:HD21	:UNL1:O	101.638
	:UNL1:H - A:GLU1046:OE1	2.19212	:UNL1:H	A:GLU1046:OE1	114.214
	:UNL1:H - A:GLU1046:OE1	2.12888	:UNL1:H	A:GLU1046:OE1	137.021
	:UNL1:H - A:VAL1039:O	2.9988	:UNL1:H	A:VAL1039:O	91.088
Kaempferol	A:ARG1072:HN - :UNL1:O	2.62735	A:ARG1072:HN	:UNL1:O	101.889
	A:GLY1073:HN - :UNL1:O	1.74046	A:GLY1073:HN	:UNL1:O	144.668
	:UNL1:H - A:VAL1039:O	2.02003	:UNL1:H	A:VAL1039:O	176.714
	:UNL1:H - A:ASP1069:OD1	2.30913	:UNL1:H	A:ASP1069:OD1	114.577
	:UNL1:H - A:GLU1046:OE1	2.04473	:UNL1:H	A:GLU1046:OE1	167.188
Naringenin	A:ARG1072:HN - :UNL1:O	2.89481	A:ARG1072:HN	:UNL1:O	97.009
	A:GLY1073:HN - :UNL1:O	1.85791	A:GLY1073:HN	:UNL1:O	158.693
	:UNL1:H - A:VAL1039:O	2.24921	:UNL1:H	A:VAL1039:O	159.885
	:UNL1:H - A:GLU1046:OE1	1.87455	:UNL1:H	A:GLU1046:OE1	135.297

Table 6. *Cont.*

Molecule	Name	Distance (A^0)	H-Donor	H-Acceptor	DHA Angle (^{0})
Isoquercetin	A:ASN1042:HD21 - :UNL1:O	2.7382	A:ASN1042:HD21	:UNL1:O	100.17
	A:ASN1042:HD21 - :UNL1:O	1.92763	A:ASN1042:HD21	:UNL1:O	164.831
	A:GLY1073:HN - :UNL1:O	1.67752	A:GLY1073:HN	:UNL1:O	141.974
	:UNL1:H - A:ASN1042:O	2.23832	:UNL1:H	A:ASN1042:O	102.23
	:UNL1:H - A:GLU1046:OE1	1.86696	:UNL1:H	A:GLU1046:OE1	133.412
	:UNL1:H - A:GLU1046:OE1	2.33954	:UNL1:H	A:GLU1046:OE1	128.18
	:UNL1:H - A:VAL1039:O	2.95873	:UNL1:H	A:VAL1039:O	103.791

Table 7. Hydrogen bonding interactions (Intermolecular Conventional Hydrogen Bond) between ligands and Topoisomerase IV ParE 24kDa subunit of *S. aureus.*

Molecule	Name	Distance (A^0)	H-Donor	H-Acceptor	DHA Angle (^{0})
Novobiocin	A:ARG138:HH11 - :UNL1:O	2.07271	A:ARG138:HH11	:UNL1:O	116.16
	:UNL1:H - A:THR92:OG1	2.30294	:UNL1:H	A:THR92:OG1	142.972
	:UNL1:H - A:GLY80:O	2.37333	:UNL1:H	A:GLY80:O	114.849
	:UNL1:H - A:GLU53:OE1	2.28073	:UNL1:H	A:GLU53:OE1	153.157
	:UNL1:H - A:ASP76:OD2	1.84227	:UNL1:H	A:ASP76:OD2	129.527
Quercetin	A:ARG79:HN - :UNL1:O	2.74275	A:ARG79:HN	:UNL1:O	97.988
	A:GLY80:HN - :UNL1:O	1.68791	A:GLY80:HN	:UNL1:O	145.046
	:UNL1:H - A:ILE46:O	2.13321	:UNL1:H	A:ILE46:O	152.776
	:UNL1:H - A:ASP76:OD1	2.27165	:UNL1:H	A:ASP76:OD1	112.554
	:UNL1:H - A:GLU53:OE2	1.92621	:UNL1:H	A:GLU53:OE2	122.031
Kaempferol	:UNL1:H - A:SER50:OG	2.19725	:UNL1:H	A:SER50:OG	150.997
	:UNL1:H - A:ASN49:O	1.75646	:UNL1:H	A:ASN49:O	133.732
	:UNL1:H - A:ASN56:OD1	1.98098	:UNL1:H	A:ASN56:OD1	144.601
	:UNL1:H - A:GLY80:O	2.00352	:UNL1:H	A:GLY80:O	143.187
Naringenin	:UNL1:H - A:GLY80:O	2.08123	:UNL1:H	A:GLY80:O	138.264
	:UNL1:H - A:ASP76:OD2	2.21723	:UNL1:H	A:ASP76:OD2	145.165
	:UNL1:H - A:THR168:O	2.91224	:UNL1:H	A:THR168:O	111.039
Isoquercetin	A:ASN49:HD21 - :UNL1:O	2.8621	A:ASN49:HD21	:UNL1:O	119.408
	:UNL1:H - A:ASN56:OD1	2.05503	:UNL1:H	A:ASN56:OD1	155.619
	:UNL1:H - A:GLU53:OE1	1.71719	:UNL1:H	A:GLU53:OE1	133.802
	:UNL1:H - A:ASN56:OD1	2.06169	:UNL1:H	A:ASN56:OD1	97.614
	:UNL1:H - A:GLU53:OE1	2.16274	:UNL1:H	A:GLU53:OE1	107.551
	:UNL1:H - A:ASP76:OD2	2.11531	:UNL1:H	A:ASP76:OD2	141.204
Sanguinarine	A:ARG79:HE - :UNL1:O	2.65739	A:ARG79:HE	:UNL1:O	90.653

Table 8. Predicted physiochemical properties of selected molecules (MW = Molecular Weight, NHA = Number of Heavy Atoms, NRB = Number of Rotatable Bonds, NHBA = Number of H-Bond Acceptors, NHBD = Number of H-Bond Donors, TPSA = Topological Polar Surface Area, O/W-PC = Octanol/Water Partition Coefficient, Lip = Lipinski's rule of five. Veb = Veber's rule, BAS = Bio-Availability Score.

Molecule	MW (g/mol)	NHA	NRB	NHBA	NHBD	TPSA (Å²)	O/W-PC (Mlogp)	Lip	Veb	BAS
Penicillin	334.39	23	5	4	2	112.01	1.55	Yes	Yes	0.56
Novobiocin	612.62	44	10	11	5	200.01	0.65	No	No	0.17
Quercetin	302.24	22	1	7	5	131.36	-0.56	Yes	Yes	0.55
Kaempferol	286.24	21	1	6	4	111.13	-0.03	Yes	Yes	0.55
Naringenin	272.25	20	1	5	3	86.99	0.71	Yes	Yes	0.55
Isoquercetin	464.38	33	4	12	8	210.51	-2.59	No	No	0.17
Lupeol	426.72	31	1	1	1	20.23	6.92	Yes	Yes	0.55
Beta-Sitosterol	414.71	30	6	1	1	20.23	6.73	Yes	Yes	0.55
Rutin	610.52	43	6	16	10	269.43	-3.89	No	No	0.17
Sanguinarine	332.33	25	0	4	0	40.80	2.72	Yes	Yes	0.55

Table 9. Predicted pharmacokinetic parameters of the selected molecules.

Pharmacokinetic parameters \ Ligand		Penicillin	Novobiocin	Quercetin	Kaempferol	Naringenin
Absorption	$CaCo_2$ permeability (log Papp in 10^{-6} cm/s)	0.114	-4.836	-0.229	0.032	1.029
	Water solubility (log mol/L)	-2.47	-0.427	-2.925	-3.04	-3.224
	Intestinal absorption (human) (% Absorbed)	59.901	66.418	77.207	74.29	91.31
	Skin Permeability (log Kp)	-2.735	-2.787	-2.735	-2.735	-2.742
	P-glycoprotein substrate	Yes	Yes	Yes	Yes	Yes
	P-glycoprotein I inhibitor	No	Yes	No	No	No
	P-glycoprotein II inhibitor	No	Yes	No	No	No
Distribution	VDss (human) (log L/kg)	-1.905	-1.336	1.559	1.274	-0.015
	Fraction unbound (human) (Fu)	0.328	0.127	0.206	0.178	0.064
	BBB permeability (log BB)	-0.864 (No)	-1.914 (No)	-1.098 (No)	-0.939 (No)	-0.578 (No)
	CNS permeability (log PS)	-2.943	-3.492	-3.065	-2.228	-2.215
Metabolism	CYP2D6 substrate	No	No	No	No	No
	CYP3A4 substrate	No	Yes	No	No	No
	CYP1A2 inhibitor	No	No	Yes	Yes	Yes
	CYP2C19 inhibitor	No	No	No	No	No
	CYP2C9 inhibitor	No	No	No	No	No
	CYP2D6 inhibitor	No	No	No	No	No
	CYP3A4 inhibitor	No	Yes	No	No	No
Excretion	Total Clearance (log ml/min/kg)	0.197	-0.228	0.407	0.477	0.06
	Renal OCT2 substrate	No	No	No	No	No
Toxicity	AMES toxicity	No	No	No	No	No
	Max. tolerated dose (human) (log mg/kg/day)	0.692	0.125	0.499	0.531	-0.176
	hERG I inhibitor	No	No	No	No	No
	hERG II inhibitor	No	Yes	No	No	No
	Oral Rat Acute Toxicity (LD50) (mol/kg)	1.716	2.085	2.471	2.449	1.791
	Oral Rat Chronic Toxicity (LOAEL) (log mg/kg_bw/day)	2.542	2.095	2.612	2.505	1.944
	Hepatotoxicity	Yes	No	No	No	No
	Skin Sensitization	No	No	No	No	No
	T. Pyriformis toxicity (log ug/L)	0.285	0.288	0.288	0.312	0.369
	Minnow toxicity (log mM)	3.698	1.146	3.721	2.885	2.136

Pharmacokinetic parameters / Ligand		Isoquercetin	Lupeol	Beta-Sitosterol	Rutin	Sanguinarine
Absorption	$CaCo_2$ permeability (log Papp in 10^{-6} cm/s)	0.242	1.226	1.201	-0.949	2.107
	Water solubility (log mol/L)	-2.925	-5.861	-6.773	-2.892	-5.56
	Intestinal absorption (human) (% Absorbed)	47.999	95.782	94.464	23.446	100
	Skin Permeability (log Kp)	-2.735	-2.744	-2.783	-2.735	-2.707
	P-glycoprotein substrate	Yes	No	No	Yes	Yes
	P-glycoprotein I inhibitor	No	Yes	Yes	No	Yes
	P-glycoprotein II inhibitor	No	Yes	Yes	No	Yes
Distribution	VDss (human) (log L/kg)	1.846	0	0.193	1.663	0.298
	Fraction unbound (human) (Fu)	0.228	0	0	0.187	0.265
	BBB permeability (log BB)	-1.688 (No)	0.726 (No)	0.781 (No)	-1.899 (No)	-0.105 (Yes)
	CNS permeability (log PS)	-4.093	-1.714	-1.705	-5.178	-1.419
Metabolism	CYP2D6 substrate	No	No	No	No	No
	CYP3A4 substrate	No	Yes	Yes	No	Yes
	CYP1A2 inhibitor	No	No	No	No	Yes
	CYP2C19 inhibitor	No	No	No	No	Yes
	CYP2C9 inhibitor	No	No	No	No	No
	CYP2D6 inhibitor	No	No	No	No	Yes
	CYP3A4 inhibitor	No	No	No	No	Yes
Excretion	Total Clearance (log ml/min/kg)	0.394	0.153	0.628	-0.369	1.051
	Renal OCT2 substrate	No	No	No	No	No
Toxicity	AMES toxicity	No	No	No	No	Yes
	Max. tolerated dose (human) (log mg/kg/day)	0.569	-0.502	-0.621	0.452	0.172
	hERG I inhibitor	No	No	No	No	No
	hERG II inhibitor	Yes	Yes	Yes	Yes	Yes
	Oral Rat Acute Toxicity (LD50) (mol/kg)	2.541	2.563	2.552	2.491	2.588
	Oral Rat Chronic Toxicity (LOAEL) (log mg/kg_bw/day)	4.417	0.89	0.855	3.673	1.729
	Hepatotoxicity	No	No	No	No	No
	Skin Sensitization	No	No	No	No	No
	T. Pyriformis toxicity (log ug/L)	0.285	0.316	0.43	0.285	0.308
	Minnow toxicity (log mM)	8.061	-1.696	-1.802	7.677	-0.718

DISCUSSION

Quercetin, Kaempferol, Naringenin, Isoquercetin, Rutin are considered as flavonoids. Lupeol is a pentacyclic triterpenoid, while Beta-Sitosterol is a Plant sterol (phytosterol). Sanguinarine belongs to Alkaloids. p-Coumaric Acid is a Hydroxycinnamic acid.

The inhibitory constant, denoted as K_i (μM), is a measurement used in pharmacology to understand how tightly a drug binds (binding affinity) to a specific molecule (target molecule). It reflects the drug concentration required to occupy half of the available binding sites. A Lower K_i value indicates stronger binding. This means a lower drug concentration sufficient to occupy half (50%) of the available binding sites. Molecules with K_i values less than 100 μM are considered potent inhibitors while molecules with higher K_i values than 100 μM are considered as non-potent inhibitors (Zheng & Polli, 2010).

Lupeol (-7.72 kcal/mol), Beta-sitosterol (-8.21 kcal/mol) show higher binding affinity to PBP 5 of *E. coli* than the Penicillin (-7.20 kcal/mol) which is the reference molecule. Both Beta-sitosterol (0.953 μM) and Lupeol (2.19 μM) show lower inhibition constant than Penicillin (5.32 μM), indicating higher potency than Penicillin (Table 2).

Quercetin (-6.85 kcal/mol), Kaempferol (-6.82 kcal/mol), Naringenin (-7.23 kcal/mol), Isoquercetin (-6.20 kcal/mol), Lupeol (-7.67 kcal/mol), Beta-Sitosterol (-9.08 kcal/mol) and Sanguinarine (-9.03 kcal/mol) show higher binding affinity to Topoisomerase IV ParE 24kDa subunit of *E. coli* than Novobiocin (-5.76 kcal/mol). Except for Beta-sitosterol, all above mentioned

molecules exhibit a lower inhibition constant than novobiocin (Table 3).

Quercetin (-6.70 kcal/mol), Kaempferol (-6.95 kcal/mol), Naringenin (-7.07 kcal/mol), Isoquercetin (-6.15 kcal/mol), Lupeol (-7.87 kcal/mol), Beta-Sitosterol (-9.42 kcal/mol) and Sanguinarine (-9.07 kcal/mol) show higher binding affinity to DNA topoisomerase IV subunit B (ParE 24kd) of *S. aureus* than novobiocin (-6.04 kcal/mol). All these molecules exhibit lower inhibition constant than novobiocin (Table 4). Among these molecules Beta-Sitosterol shows the highest binding affinity and the lowest inhibition constant towards Topoisomerase IV ParE 24kDa subunit of *S. aureus.*

Interactions between a ligand and a protein are crucial for understanding biochemical processes, particularly in protein function and stability. Two major types of interactions that can be observed are hydrogen bonds (H-bonds) and hydrophobic interactions. Hydrogen bonds significantly contribute to the stability of the protein structure. Furthermore, H-bonds can provide specificity in ligand binding. The precise arrangement of H-bond donors and acceptors facilitates selective binding of ligands. Higher the number of H-bonds, greater the binding efficiency and the inhibition (Kumar et al., 2015). Hydrophobic interactions drive protein folding and significantly contribute to the stability of the protein.

In H-bond interactions analysis, Penicillin forms three H-bonds with three amino acids (SER44, SER87, and ASN112) located in the active site of the PBP5. In the case of PBP5 and Lupeol one H-bonding interaction was observed (SER44), while PBP5 and Beta-sitosterol exhibit one H-bond (ASN112) (Figure 3 and Table 5).

Two H-bonds were observed between the Topoisomerase IV ParE 24kDa subunit of *E. coli* and novobiocin (HIS1079 and ILE1078). Additionally, quercetin forms four H-bonds with three amino acids (ASN1042, GLU1046 and VAL1039) in the active site of this protein. Five H-bonds with five amino acids in the active site, were observed between kaempferol and the protein (ARG1072, GLY1073, VAL1039, ASO1069 and GLU1046). Similarly, four H-bonds with four amino acids in the active site, were observed between naringenin and the protein (ARG1072, GLY1073, VAL1039 and GLU1046). The highest number of H-bonds was observed between Isoquercetin and the protein, seven H-bonds with four amino acids in the active site (ASN1042, GLY1073, GLU1046 and VAL1039). Lupeol, beta-sitosterol and sanguinarine do not form H-bonds with the Topoisomerase IV ParE 24kDa subunit of *E. coli,* but they exhibit hydrophobic interactions with the protein (Figure 4 and Table 6).

Considering the H-bonds between Topoisomerase IV ParE 24kDa subunit of *S. aureus* and novobiocin, five H-bonds were observed with five amino acids present in the active site (ARG138, THR92, GLY80, GLU53 and ASP76). Between quercetin and the protein, five H-bonds with five amino acids present on the active site, were observed (ARG79, GLY80, ILE46, ASP76, and GLU53). Kaempferol shows four H-bonds with the protein (SER50, ASN49, ASN56, and GLY80). Three H-bonds were observed between the protein and naringenin (GLY80, ASP76, and THR168). The highest number of H-bonds observed is six between Isoquercetin and the protein (ASN49, ASN56, GLU53, and ASP76). Sanguinarine exhibits one H-bond with the protein (ARG79). Both lupeol and beta-sitosterol show hydrophilic interactions with the protein but do not form any H-bonds (Figure 5 and Table 7).

Considering the predicted physiochemical properties of selected molecules, Isoquercetin and Rutin do not fulfil Lipinski's and Veber's rules. Even novobiocin, a commercially available antibiotic, does not fulfil Lipinski's and Veber's rules. Except for Sanguinarine, none penetrates the Blood brain barrier (BBB). Oral rat acute toxicity (LD50) is defined as the amount of substance that is required to kill 50% of a tested population within a specific time frame. Among the selected molecules, all except Naringenin exhibit higher LD50 values compared to commercially available antibiotics which are Penicillin and Novobiocin. A higher LD50 value suggests that these molecules may be less toxic than Penicillin and Novobiocin. Hepatotoxicity which is also known as liver toxicity of the selected molecules was also evaluated. All the molecules, except Penicillin, were found to be non-hepatotoxic.

When considering the number of selected molecules that exhibit higher binding affinity to the protein than the reference molecule, only two molecules (Lupeol and Beta-sitosterol) exhibit higher binding affinity than penicillin against PBP 5 of *E. coli*. In the case of Topoisomerase IV ParE 24kDa subunit, seven molecules exhibit higher binding affinity compared to the reference molecule which is novobiocin in both *E. coli* and *S. aureus*. Further studies should be conducted to investigate the combined effect of the molecules against each protein.

These results reveal that selected phytochemicals show a higher inhibitory effect on the DNA Topoisomerase IV ParE 24kDa subunit compared to their effect on PBP5. This suggests that selected molecules may inhibit enzymes crucial to bacterial structural component synthesis and DNA replication. These molecules may exhibit a dual mechanism of action. This dual action mechanism may potentially kill or reduce the growth of microorganisms.

The re-docking was done to validate the docking procedure. Penicillin bound to the active site of the Penicillin-binding protein 5 of *E. coli* with binding energy of -7.20 kcal/mol. Penicillin formed three H-bonds with three amino acids (SER44, SER87, and ASN112) located in the active site of the PBP 5 of *E. coli* with a distance ranging from 1.7 – 2.1 A^0. These bonds are well within the optimal range for H-bonding, indicating a strong interaction. The re-docked complex

was then superimposed on to the native crystalized structure of *E. coli* PBP 5 from PDB using PyMOL observed 0.000 A^0 RMSD value. The same methodology was followed for both Topoisomerase IV ParE 24kDa subunit of *E. coli* and *S. aureus* with novobiocin. Novobiocin formed two H-bonds with two amino acids (HIS1079 and ILE1078) located in the active site of the Topoisomerase IV ParE 24kDa subunit of *E. coli* with a distance ranging from 2.4 – 2.9 A^0. Novobiocin formed five H-bonds with five amino acids (ARG138, THR92, GLY80, GLU53, and ASP76) located in the active site of the Topoisomerase IV ParE 24kDa subunit of *S. aureus* with a distance ranging from 1.8 – 2.4 A^0. These bonds are well within the optimal range for H-bonding, indicating a strong interaction. The re-docked complexes were then superimposed on to their native crystalized structures using PyMOL and observed 0.000 A^0 RMSD value (Figure 2). Obtaining 0.000 A^0 for RMSD indicates no difference between the re-docked complex and the referenced crystallized structure.

Overall, this study provides a strong foundation for further investigations to study anti-microbial activity of selected molecules derived from phytochemicals of *Coccinia grandis* leaves. These findings may pave the way for developing novel antibiotic agents with enhanced inhibitory efficacy.

CONCLUSION

Selected phytochemicals of *Coccinia grandis* leaves were evaluated *in silico* to determine their antimicrobial activity against Penicillin-binding protein 5 (PBP 5) and Topoisomerase IV ParE 24kDa subunit of *Escherichia coli* and Topoisomerase IV ParE 24kDa subunit of *Staphylococcus aureus*. Physiochemical and pharmacokinetic properties of selected molecules were also evaluated. Molecular docking, physiochemical and pharmacokinetic results were compared with reference molecules which are Penicillin and Novobiocin which are commercially available antibiotics.

Out of the tested molecules, Lupeol and Beta-sitosterol exhibited better inhibition capabilities against PBP5 of *Escherichia coli* than Penicillin. Quercetin, Kaempferol, Naringenin, Isoquercetin, Lupeol, Beta-Sitosterol and Sanguinarine exhibit higher binding affinity to Topoisomerase IV ParE 24kDa subunit of both *Escherichia coli* and *Staphylococcus aureus* than Novobiocin. Selected natural molecules exhibit higher binding affinity towards Topoisomerase IV ParE 24kDa subunit than PBP5 of *E. coli*.

Results in this study suggest that these selected phytochemicals of *Coccinia grandis* Leaves may serve as promising candidates for development of antimicrobial agents against resistant strains of *Escherichia coli* and *Staphylococcus aureus.* Further studies should focus on optimizing the structure of these selected molecules to enhance their binding affinity and the inhibitory potency.

Acknowledgements: I would like to express my sincere gratitude to Dr. M.G.A.N. Perera from the faculty of Applied Science at the University of Sabaragamuwa for his invaluable guidance and support throughout this research.

Authors' Contributions: M. Isuranga designed the study. Computational analysis and data interpretation were conducted by M. Isuranga and D.N. Danthanarayana. The manuscript was written by both M. Isuranga and D.N. Danthanarayana.

Competing Interests: The author declares that there are no competing interests.

REFERENCES

Bellon, S., Parsons, J. D., Wei, Y., Hayakawa, K., Swenson, L. L., Charifson, P. S., Lippke, J. A., Aldape, R., & Gross, C. H. (2004). Crystal Structures of Escherichia coli Topoisomerase IV ParE Subunit (24 and 43 Kilodaltons): A Single Residue Dictates Differences in Novobiocin Potency against Topoisomerase IV and DNA Gyrase. *Antimicrobial Agents and Chemotherapy*, *48*(5), 1856–1864. https://doi.org/10.1128/AAC.48.5.1856-1864.2004

Farrukh, U., Shareef, H., & ayub Ali, syed. (2008). *Antibacterial activities of Coccinia grandis L.* https://www.researchgate.net/publication/230795441

Global Antimicrobial Resistance and Use Surveillance System (GLASS) Report 2022. (2022). World Health Organization.

Kumar, K., Kumar, S. R., Dwivedi, V., Rai, A., Shukla, A. K., Shanker, K., & Nagegowda, D. A. (2015). Precursor feeding studies and molecular characterization of geraniol synthase establish the limiting role of geraniol in monoterpene indole alkaloid biosynthesis in Catharanthus roseus leaves. *Plant Science*, *239*, 56–66. https://doi.org/10.1016/j.plantsci.2015.07.007

Larsson, D. G. J., & Flach, C. F. (2022). Antibiotic resistance in the environment. In *Nature Reviews Microbiology* (Vol. 20, Issue 5, pp. 257–269). Nature Research. https://doi.org/10.1038/s41579-021-00649-x

Lawan, H., & Tharakee, H. (2023). In silico Study on Structural Inhibition of Bacterial DNA Gyrase by Major Secondary Metabolites Found in Grape Seed Extract. *Biology, Medicine, & Natural Product Chemistry*, *12*(2), 585–592. https://doi.org/10.14421/biomedich.2023.122.585-592

Lipinski, C. A., Lombardo, F., Dominy, B. W., & Feeney, P. J. (2001). Experimental and computational approaches to estimate solubility and permeability in drug discovery and development q settings. In *Advanced Drug Delivery Reviews* (Vol. 46). www.elsevier.com/locate/drugdeliv

Lu, J., Patel, S., Sharma, N., Soisson, S. M., Kishii, R., Takei, M., Fukuda, Y., Lumb, K. J., & Singh, S. B. (2014b). Structures of kibdelomycin bound to Staphylococcus aureus GyrB and ParE showed a novel U-shaped binding mode. *ACS Chemical Biology*, *9*(9), 2023–2031. https://doi.org/10.1021/cb5001197

Nicholas, R. A., Krings, S., Tomberg, J., Nicola, G., & Davies, C. (2003). Crystal structure of wild-type penicillin-binding protein 5 from Escherichia coli: Implications for deacylation of the acyl-enzyme complex. *Journal of Biological Chemistry*,

278(52), 52826–52833. https://doi.org/10.1074/jbc.M310177200

Ramachandran, A., Prasath, R., & Anand, A. (2014). THE MEDICAL USES OF COCCINIA GRANDIS L. VOIGT: A REVIEW. *International Journal of Pharmacognosy*, *1*(11), 681–690. https://doi.org/10.13040/IJPSR.0975-8232.IJP.1(11).681-90

Sauvage, E., Powell, A. J., Heilemann, J., Josephine, H. R., Charlier, P., Davies, C., & Pratt, R. F. (2008). Crystal Structures of Complexes of Bacterial dd-Peptidases with Peptidoglycan-Mimetic Ligands: The Substrate Specificity Puzzle. *Journal of Molecular Biology*, *381*(2), 383–393. https://doi.org/10.1016/j.jmb.2008.06.012

Shivanika, C., Deepak Kumar, S., Ragunathan, V., Tiwari, P., Sumitha, A., & Brindha Devi, P. (2022). Molecular docking, validation, dynamics simulations, and pharmacokinetic prediction of natural compounds against the SARS-CoV-2 main-protease. *Journal of Biomolecular Structure and Dynamics*, *40*(2), 585–611. https://doi.org/10.1080/07391102.2020.1815584

Veber, D. F., Johnson, S. R., Cheng, H. Y., Smith, B. R., Ward, K. W., & Kopple, K. D. (2002). Molecular properties that influence the oral bioavailability of drug candidates. *Journal of Medicinal Chemistry*, *45*(12), 2615–2623. https://doi.org/10.1021/jm020017n

Zhang, W., Shi, Q., Meroueh, S. O., Vakulenko, S. B., & Mobashery, S. (2007). Catalytic mechanism of penicillin-binding protein 5 of Escherichia coli. *Biochemistry*, *46*(35), 10113–10121. https://doi.org/10.1021/bi700777x

Zheng, X., & Polli, J. (2010). Identification of inhibitor concentrations to efficiently screen and measure inhibition Ki values against solute carrier transporters. *European Journal of Pharmaceutical Sciences*, *41*(1), 43–52. https://doi.org/10.1016/j.ejps.2010.05.013